Ammonium, barium hexacyanoferrate(II) trihydrate

Lucrecia Medina Córdoba, Gustavo A. Echeverría, Oscar E. Piro & M. Inés Gómez

Journal of Thermal Analysis and Calorimetry
An International Forum for Thermal Studies

ISSN 1388-6150
Volume 120
Number 3

J Therm Anal Calorim (2015)
120:1827-1834
DOI 10.1007/s10973-015-4492-5

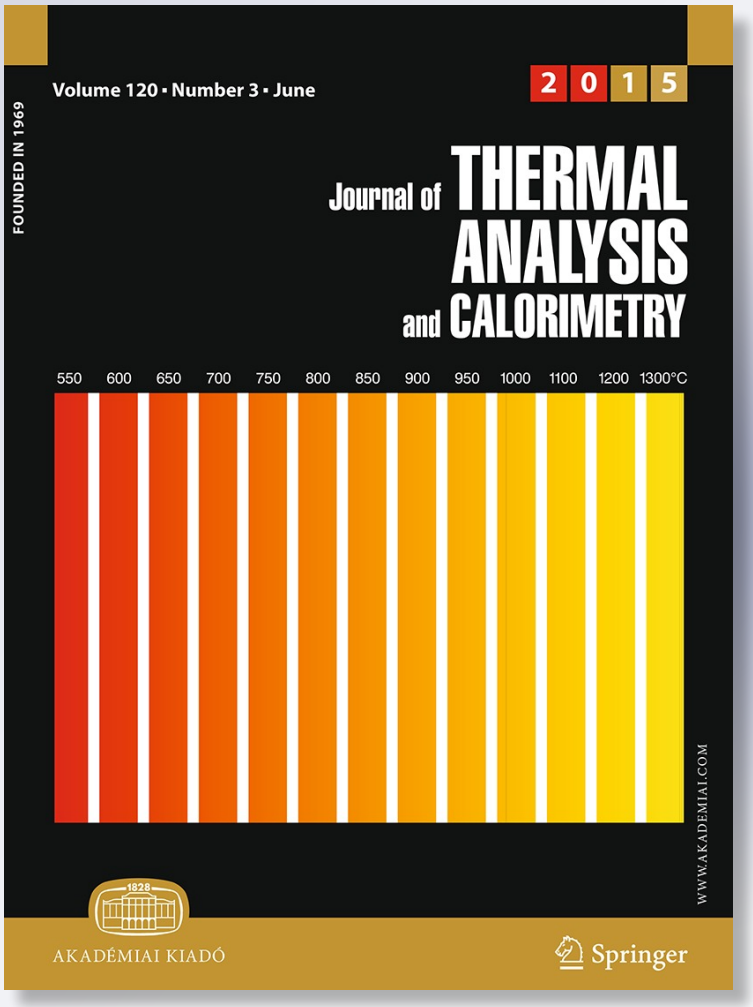

Springer

J Therm Anal Calorim (2015) 120:1827–1834
DOI 10.1007/s10973-015-4492-5

Ammonium, barium hexacyanoferrate(II) trihydrate

Synthesis, crystal structure, thermal decomposition and spectroscopic study

Lucrecia Medina Córdoba · Gustavo A. Echeverría · Oscar E. Piro · M. Inés Gómez

Received: 3 September 2014 / Accepted: 23 January 2015 / Published online: 18 February 2015

Abstract The ammonium, barium hexacyanoferrate(II) trihydrate, $Ba(NH_4)_2[Fe(CN)_6]\cdot 3H_2O$, has been synthesized for the first time, was characterized by thermogravimetric and differential thermal analysis (TG–DTA), infrared (IR) and Raman spectroscopy and chemical analysis, and its crystal and molecular structures were determined by X-ray diffraction methods. The chemical composition was determined by assaying Ba(II) with EDTA, ammonia nitrogen with Nessler's reagent as indicator and Fe(II) using spectrophotometry with ortho-phenanthroline method. The hydration number was estimated by thermogravimetric analysis. The compound crystallizes in the trigonal *R*-3*c* space group. The ferrocyanide anion has an almost perfect octahedral shape with its Fe(II) ion in a crystallographic special position of point symmetry S_6 [d(Fe–C) = 1.912(2) Å, d(C–N) = 1.153(3) Å]. The barium, ammonium nitrogen and water oxygen atoms are also at lattice special positions with site symmetries D_3, C_3 and C_2, respectively. The thermal decomposition process was also studied using TG–DTA, and the products of decomposition were identified by IR spectroscopy. It proposes a mechanism of decomposition.

Keywords Ferrocyanide · Synthesis · Thermal analysis · Crystal structure · IR spectroscopy

Introduction

The study of cyanocomplexes has received much attention for a long time because they are important precursors for the synthesis of perovskite-type oxides which have a variety of applications such as chemical sensors and catalysts [1–4]. It is also well known that it can be used in organometallic and coordination chemistry for the synthesis of various super-complexes or molecular assemblies and also in the field of supramolecular chemistry to build various 1D, 2D or 3D structures [5–9].

Most of their applications are based on the ability of the cyano groups to bind several metal centers. Among their many applications, these complexes can act as catalysts, chemical sensors, molecular sieves for storing gases, photosensitizers and prototypes of molecular magnets [10–13].

In previous researches, the hexacyano and pentacyano nitrosyl complexes have been used as precursors to prepare mixed oxides from the thermal decomposition in oxidative atmosphere. It was shown that this method produced compounds with a high superficial area, which determines the potential catalytic activity of the products [14–17]. In addition, the complexes and their decomposition products have interesting solid state properties because they exhibit the coexistence of ferroelectric and magnetic behavior [18]. Recently, the magnetic properties of yttrium hexacyanoferrate and the series of $Y[Fe_{1-x}Co_x(CN)_6]\cdot 4H_2O$ ($0 < x < 1$) solid solutions have been studied by Gil et al. The obtained oxides from the thermal decomposition of the complexes also have interesting electric and magnetocaloric properties [19–21].

Electronic supplementary material The online version of this article (doi:10.1007/s10973-015-4492-5) contains supplementary material, which is available to authorized users.

L. M. Córdoba · M. I. Gómez (✉)
Instituto de Química Inorgánica, Facultad de Bioquímica, Química y Farmacia, Universidad Nacional de Tucumán, Ayacucho 471, T4000INI San Miguel de Tucumán, Argentina
e-mail: mgomez@fbqf.unt.edu.ar

G. A. Echeverría · O. E. Piro
Departamento de Física and Institute IFLP (CONICET, CCT-La Plata), Facultad de Ciencias Exactas, Universidad Nacional de La Plata, C. C. 67, 1900 La Plata, Argentina

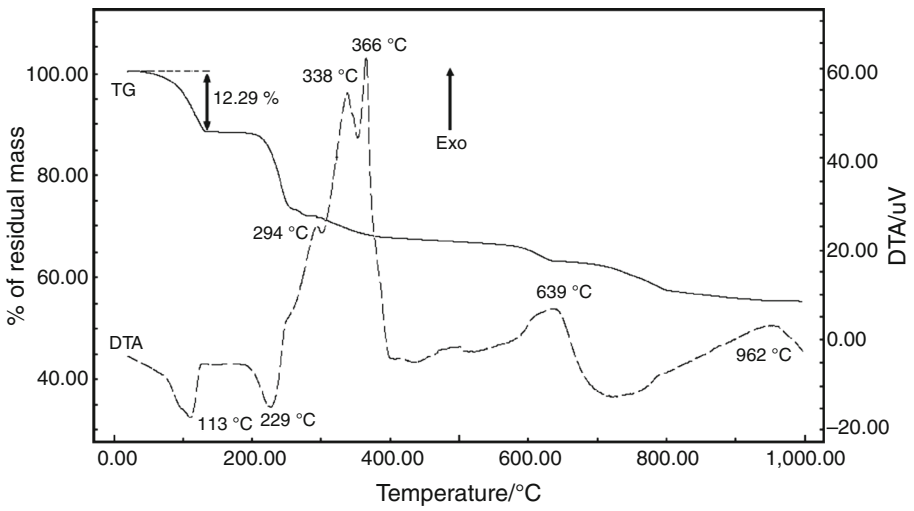

Fig. 1 TG and DTA curves for $Ba(NH_4)_2[Fe(CN)_6]\cdot 3H_2O$ in air

Table 1 Crystal data and structure refinement results for $Ba(NH_4)_2[Fe(CN)_6]\cdot 3H_2O$

Empirical formula	$C_6H_{14}BaFeN_8O_3$
Formula weight	439.44
Temperature	295(2) K
Wavelength	0.71073 Å
Crystal system	Trigonal
Space group	*R*-3*c* (#167)
Unit cell dimensions	$a = 7.3744(2)$ Å
	$b = 7.3744(2)$ Å
	$c = 4.5758(2)$ Å
Volume	2,155.0(1) $Å^3$
Z, Density (calculated)	6, 2.032 mg m^{-3}
Absorption coefficient	3.751 mm^{-1}
F(000)	1,272
Crystal size	$0.14 \times 0.12 \times 0.08$ mm^3
Crystal shape/color	Prism/light yellow
ϑ–range for data collection	3.31°–26.50°
Index ranges	$-9 \le h \le 7$, $-5 \le k \le 9$, $-57 \le l \le 57$
Reflections collected	2,728
Independent reflections	504 [R(int) = 0.022]
Observed reflections [$I > 2\sigma(I)$]	451
Completeness to $\vartheta = 26.50°$	99.8 %
Max. and min. transmission	0.7535 and 0.6237
Refinement method	Full-matrix least-squares on F^2
Data/restraints/parameters	504/3/42
Goodness-of-fit on F^2	1.135
Final R^a indices [$I > 2\sigma(I)$]	$R_1 = 0.0160$, $wR_2 = 0.0427$
R indices (all data)	$R_1 = 0.0187$, $wR_2 = 0.0442$
Extinction coefficient	0.00078(9)
Largest diff. peak and hole	0.488 and −0.443 e.$Å^{-3}$

[a] $R_1 = \Sigma||F_o|-|F_c||/\Sigma|F_o|, wR_2 = \left[\Sigma w\left(|F_o|^2-|F_c|^2\right)^2/\Sigma w\left(|F_o|^2\right)^2\right]^{1/2}$

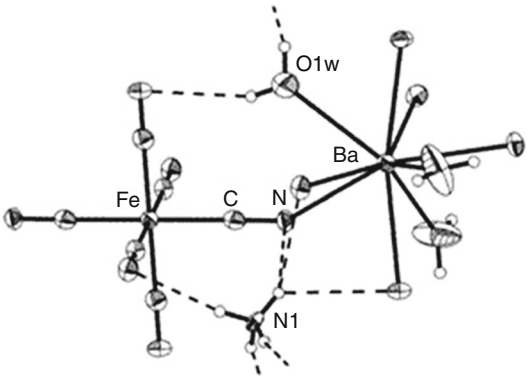

Fig. 2 Plot of $Ba(NH_4)_2[Fe(CN)_6]\cdot 3H_2O$ showing the labeling of the independent non-H atoms and their displacement ellipsoids at the 50 % probability level. Unlabeled hatched ellipsoids around barium are cyanide N atoms of neighboring, symmetry related, $[Fe(CN)_6]^{4-}$ complexes. H bonds are indicated by dashed lines. Iron, barium, ammonium nitrogen, and water oxygen atoms are at crystallographic special positions of point symmetries S_6, D_3, C_3 and C_2, respectively

Table 2 Bond lengths [Å] and angles [°] for $Ba(NH_4)_2[Fe(CN)_6]\cdot 3H_2O$

C–N	1.153(3)	O(1W)–Ba–N#2	134.02(4)
C–Fe	1.912(2)	O(1W)–Ba–N#3	74.16(4)
N–Ba	2.894(2)	O(1W)–Ba–N	65.04(4)
Ba–O(1W)	2.880(3)	N#3-Ba–N	74.66(7)
N–C–Fe	178.6(2)	N–Ba–N#4	130.08(8)
C–N–Ba	146.3(2)	N–Ba–N#5	148.33(8)
C#1-Fe–C	90.53(8)	N–Ba–N#6	91.97(9)

Symmetry transformations used to generate equivalent atoms

(#1) $-y, x-y-1, z$; (#2) $-y+1, x-y, z$; (#3) $-x+y+1, -x+1, z$; (#4) $y+1/3, x-1/3, -z+1/6$; (#5) $x-y+1/3, -y+2/3, -z+1/6$; (#6) $-x+4/3, -x+y+2/3, -z+1/6$

The crystal structures of some hexacyanoferrates and mixed metal ferrocyanides have been reported previously. In 1973, Bailey et al. [22] determined the crystal structure of $La[Fe(CN)_6]\cdot 5H_2O$ by single-crystal X-ray diffraction analysis, which was later confirmed by Kietaibl and Bonnet [23–25]. Other authors determined the crystal structure of yttrium hexacyanoferrate(III) and bismuth hexacyanoferrate(III) by Rietveld analysis of powder X-ray diffraction data [20, 26–28].

In 1977, Raistrick et al. [29] determined the crystal structure of some mixed metal hexacyanoferrates of the type $A_2B[Fe(CN)_6]\cdot xH_2O$ (where A = alkali metal, ammonium and B = divalent metal). If A = ammonium and B = Mg(II), the crystal symmetry is cubic, while for A = ammonium and B = Ca(II), the symmetry reduces to tetragonal.

We have already reported the crystal structure of ammonium, strontium hexacyanoferrate(II) dihydrate. It crystallizes in the orthorhombic *Pnma* space group [30].

The thermal decomposition of hetero-nuclear complexes was proposed by Gallagher [31] in 1968 to prepare $LaFeO_3$ and $LaCoO_3$ using hexacyanometallates as precursors. The oxides obtained by this method were formed at shorter times and lower temperatures than ceramic methods. In addition, the use of soft chemical routes can yield homogeneous phases with small grain size, a feature which improves the catalytic properties [16, 17, 20, 26, 28, 31–34].

In this work, we report the synthesis, thermal analysis, spectroscopic properties and crystal structure of a new ammonium, barium hexacyanoferrate(II) trihydrate. The techniques used were thermogravimetric and differential thermal analysis (TG–DTA), infrared (IR) and Raman spectroscopy and structural single-crystal X-ray diffraction analysis.

Experimental

Synthesis

$Ba(NH_4)_2[Fe(CN)_6]$ was prepared by mixing equal volumes of 20 mmol of sodium hexacyanoferrate(II) decahydrate, 40 mmol ammonium chloride and 20 mmol barium chloride in an inert atmosphere. The addition of $BaCl_2$ was done in stages until the calculated amount was reached [35].

The reaction that takes place can be represented by the following equation:

$$[Fe(CN)_6]^{4-} + 2\,NH_4^+ + Ba^{2+} \Rightarrow \underset{\text{Light yellow}}{Ba(NH_4)_2[Fe\,(CN)_6]} \downarrow \quad (1)$$

The obtained precipitate was filtered out from the solution under vacuum and then stored in a dry box with silica gel.

The chemical composition of the substance was determined by assaying Ba(II) using EDTA, ammonia nitrogen using Nessler's reagent as indicator and Fe(II) using spectrophotometry with *o*-phenanthroline method [36–38]. The water content was determined by thermogravimetric analysis (TG) with a Shimadzu TG-50 equipment at 5° min^{-1} under flowing air.

Characterization

Thermogravimetric and differential thermal analysis (TG–DTA) measurements were performed with a Shimadzu TG/DTA-50 from room temperature (RT) to 1,000 °C at a heating rate of 5° min^{-1} under flowing air.

Infrared absorption spectra (in the 4,000–400 cm^{-1} region) were recorded at RT on a FTIR Perkin-Elmer 1600

Table 3 Steps for the thermal decomposition of $Ba(NH_4)_2[Fe(CN)_6]\cdot 3H_2O$ and % of mass loss

Step	Temperature range/°C	Observed mass loss/%	Theoretical mass loss/%
1	20–140	12.29	12.30
2	180–400	20.44	20.04
3	400–650	5.17	4.55
4	650–1,000	7.07	8.02
Total mass loss/%		44.96	44.91

spectrophotometer in the transmission mode using KBr pellets.

The measurements of X-ray diffraction were performed on an Oxford Xcalibur Gemini, Eos CCD diffractometer with graphite-monochromated MoKα ($\lambda = 0.71073$ Å) radiation. X-ray diffraction intensities were collected (ω scans with ϑ and κ-offsets), integrated and scaled with CrysAlisPro [39] suite of programs. The unit cell parameters were obtained by least-squares refinement (based on the angular settings for all collected reflections with intensities larger than seven times the standard deviation of measurement errors). Data were corrected empirically for absorption employing the multi-scan method implemented in CrysAlisPro. The structure was solved by direct methods with SHELXS-97 of the SHELX suite of programs [40] and the molecular model refined by full-matrix least-squares procedure with SHELXL-97 of the same package.

The ammonium and water hydrogen atoms were located in a difference Fourier map phased on the heavier atoms and refined at their found positions with isotropic displacement parameters and the N–H and Ow–H bond distances constrained to a target value of 0.86(1) Å.

Results and discussion

Chemical analysis

The crystals of ammonium barium hexacyanoferrate(II) have pinacoidal morphology [41]. Their mean size was in the range from 7 to 12 mm.

Ba(II), Fe(II) and NH_4^+ were analyzed by analytical techniques and the number of water molecules was calculated from TG measurements (see Fig. 1). The dehydration process ends at 140 °C, and the mass loss was 12.29 %. This corresponds to the elimination of three water molecules (theoretical value 12.30 %).

Anal. Calcd. for $Ba(NH_4)_2[Fe(CN)_6]\cdot 3H_2O$ (%): Ba, 31.29; Fe, 12.67; NH_4^+, 6.38; H_2O, 12.30. *Found:* Ba, 30.76; Fe, 12.11; NH_4^+, 6.06; H_2O, 12.29.

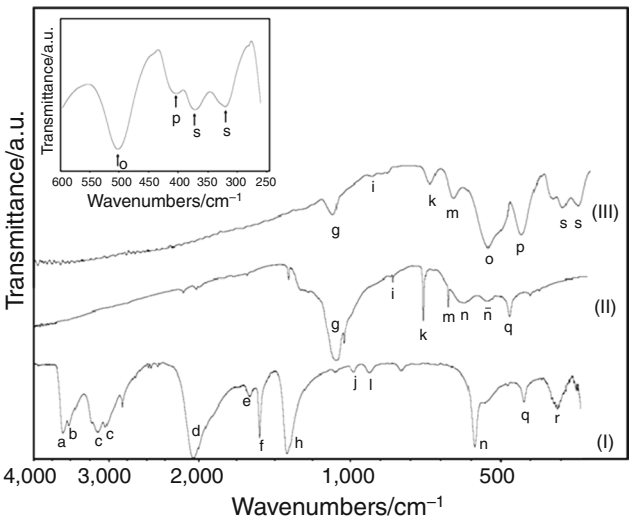

Fig. 3 IR spectra of $Ba(NH_4)_2[Fe(CN)_6]\cdot 3H_2O$ and its thermal decomposition products: *I* RT, *II* 450 °C and *III* 1,000 °C. *Inset*: IR spectrum between 600 and 250 cm^{-1} at 1,000 °C

Crystal structure

$Ba(NH_4)_2[Fe(CN)_6]\cdot 3H_2O$ crystallizes in the trigonal *R*-3*c* space group (in the hexagonal setting) with $a = b = 7.3744(2)$, $c = 45.758(2)$ Å and $Z = 6$ molecules per unit cell. The ferrocyanide complex is center symmetric with its Fe(II) ion sited on a special position with point symmetry S_6 ($\bar{3}$) in a nearly perfect octahedral environment. The metal is sixfold coordinated by the C atom of the cyanide ligand [d(Fe–C) = 1.912(2) Å, d(C–N) = 1.153(3) Å and Fe–C–N angle of 178.6(2)°]. *Cis* C–Fe–C bond angles depart from perfect perpendicularity in 0.53(8)°. The Ba(II) ion is located on a crystallographic D_3 point symmetry in a ninefold environment. It is coordinated by six cyanide groups conforming an Archimedean triangular anti-prism geometry where the metal is sandwiched between two triangular basis with a cyanide N atom at each vertex [d(Ba–N) = 2.894(2) Å], rotated in 14.12(7)° from each other. The ninefold environment around barium is completed by three symmetry-related water molecules [d(Ba–O1w) = 2.880(3) Å] entering equatorial coordination along the C_2 axes of the D_3 point group. The ammonium cation is sited on a crystallographic threefold rotation axis (site symmetry C_3).

The lattice presents weak H bonds involving the ammonium ion and the water molecule as donors and the cyanide N atom as acceptor [$N\cdots N_{cy}$ distances of 3.039 and 3.308 Å and $N–H\cdots N_{cyan}$ angles of 161.25° and 131.05°, respectively, and $d(Ow\cdots N_{cyan}) = 3.240$ Å and angle $(Ow–H\cdots N_{cyan}) = 149.18°$]. Further details of the H-bonding structure are provided as supplementary information.

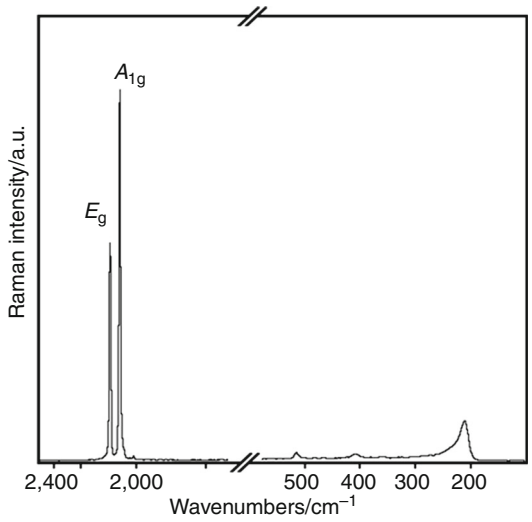

Fig. 4 Raman spectrum of $Ba(NH_4)_2[Fe(CN)_6]\cdot 3H_2O$

The crystal structure of $Ba(NH_4)_2[Fe(CN)_6]\cdot 3H_2O$ can be compared with the related $Sr(NH_4)_2[Fe(CN)_6]\cdot 2H_2O$ compound [30]. The strontium complex crystallizes in the orthorhombic space group *Pnma* with the ferrocyanide complex on an inversion center and the Sr(II) ion sited on a crystallographic mirror plane (Cs) in an eightfold Archimedean square anti-prism coordination. The corners across the diagonals of each square basis are occupied by water molecules (on Cs sites) and cyanide N atoms. The ammonium molecule is at a crystal general position.

Crystal data and structure refinement results are summarized in Table 1. Figure 2 shows an ORTEP [42] plot of $Ba(NH_4)_2[Fe(CN)_6]\cdot 3H_2O$, and distances and angles bond are given in Table 2.

Thermal decomposition

The thermal behavior of $Ba(NH_4)_2[Fe(CN)_6]\cdot 3H_2O$ in air was studied by TG and DTA (see Fig. 1). The first step in TG curve ends at 140 °C with mass loss of 12.29 %, which can be attributed to the elimination of three water molecules per chemical formula. This corresponds with the endothermic DTA peak observed at 113 °C. The second step begins at 180 °C and ends at 400 °C with a mass loss

Table 4 Frequencies (cm^{-1}) and assignments of bands in the infrared (at different temperatures) and Raman (at RT) spectra of $Ba(NH_4)_2[Fe(CN)_6]\cdot 3H_2O$

IR			Raman (RT)	Assignment	Ref.
Room temperature	450 °C	1,000 °C			
3,622	–	–	–	ν_1OH coordinate water	(a)
3,545	–	–	–	ν_3OH coordinate water	(b)
3,146–3,062	–	–	–	$\nu_3NH_4^+$	(c)
–	–	–	2,095	ν_sCN^-	
–	–	–	2,060	ν_sCN^-	
2,041	–	–	–	ν_3CN^-	(d)
1,669	–	–	–	$\nu_2NH_4^+$	(e)
1,607	–	–	–	δ(HOH) coordinate water	(f)
–	1,437	1,447	–	ν_3 [CO_3^{2-}]	(g)
1,418	–	–	–	δHNH	(h)
–	1,086(vw)	1,078(vw)	–	ν_1 [CO_3^{2-}]	(i)
998–941	–	–	–	ρH_2O	(j)
–	857	856	–	δ [CO_3^{2-}]	(k)
830	–	–	–	ωH_2O	(l)
–	686	661	–	ν_4 [CO_3^{2-}]	(m)
585	571	–	–	ν [FeC]	(n)
–	557	–	–	ν [BaC]	(ñ)
–	–	571	–	Fe_2O_3	(o)
–	–	500	–	$BaFeO_{2,5}$	(p)
414	471	–	518	δFeCN	(q)
			416	ν_sCFeC	
386	–	–	–	δFeC	(r)
–	–	373–303	–	δOFeO	(s)
–	–	–	208	?	

of 20.44 %, and it is assigned to the elimination of two ammonium cyanide molecules and the formation of iron(II) cyanide and barium cyanide. In DTA are observed one endothermic peak at 229 °C and three exothermic ones at 294, 338 and 366 °C. The third decomposition step occurs in the 400–650 °C range and is attributed to the loss of NO and elimination and oxidation (exothermic combustion) of the CN groups with the simultaneous formation of barium carbonate and ferric oxide [15, 26]. In DTA, this process appears as an exothermic peak at 639 °C. Finally, for the last stage of decomposition (650–1,000 °C range), it can be assumed that part of barium carbonate is decomposed to generate $BaFeO_{2.5}$ mixed oxide leaving a small residue of barium carbonate, as expected because the decomposition temperature of $BaCO_3$ is 1,450 °C [43]. Other authors have previously reported that very prolonged warming is required to obtain samples free of carbonates in the synthesis of mixed oxides of strontium and barium [14, 15, 17, 26, 44]. In DTA is observed an exothermic peak at 962 °C. The expected mass losses in each of the decomposition steps are in good agreement with the experimental values. These results are summarized in Table 3. The total mass loss from RT to 1,000 °C is 44.96 %. This is in agreement with the theoretical mass loss (44.91 %) for the formation of $BaFeO_{2.5}$ from the complex.

The sequence of decomposition steps could be expressed as:

$$Ba(NH_4)_2[Fe(CN)_6]\cdot 3H_2O_{(s)}\ \emptyset \Rightarrow Ba(NH_4)_2[Fe(CN)_6]_{(s)} + 3\,H_2O_{(g)} \quad (2)$$

$$Ba(NH_4)_2[Fe(CN)_6]_{(s)}\ \emptyset \Rightarrow Fe(CN)_{2(s)} + Ba(CN)_{2(s)} + 2\,NH_4CN_{(g)} \quad (3)$$

$$Fe(CN)_{2(s)} + Ba(CN)_{2(s)} + \frac{11}{2}O_{2(g)}\ \emptyset \Rightarrow BaCO_{3(s)} + \frac{1}{2}Fe_2O_{3(s)} + \frac{3}{2}(CN)_{2(g)} + NO_{(g)} \quad (4)$$

$$BaCO_{3(s)} + \frac{1}{2}Fe_2O_{3(s)}\ \emptyset \Rightarrow BaFeO_{2.5(s)} + CO_{2(g)} \quad (5)$$

The complete reaction can be written as:

$$Ba(NH_4)_2[Fe(CN)_6]\cdot 3H_2O_{(s)} + \frac{11}{2}O_{2(g)}\ \theta \Rightarrow BaFeO_{2.5(s)} + 3H_2O_{(g)} + 2\,NH_4CN_{(g)} + \frac{3}{2}(CN)_{2(g)} + NO_{(g)} + CO_{2(g)} \quad (6)$$

Vibrational analysis

We analyzed the vibrational behavior of the complex by IR spectroscopy and the results are shown in Fig. 3 (I). At RT, the absorption bands observed at 2,045, 585 and 414 cm^{-1} are assigned to the ν_3(CN) stretching, ν(FeC) stretching and δ(FeCN) bending modes, respectively. Two IR bands appear at 3,622 and 3,545 cm^{-1} due to the H_2O asymmetric (ν_1) and symmetric (ν_3) stretching modes, respectively, and a single and narrow band at 1,607 cm^{-1} is assigned to the δ(HOH) deformation [45]. It was also observed the rocking mode $\rho(H_2O)$ at 998 and 941 cm^{-1} and wagging vibrations $\omega(H_2O)$ at 830 cm^{-1}. The bands located between 3,146 and 3,062 cm^{-1} are due to ammonium stretching modes $\nu_3(NH_4^+)$, while NH_4^+ deformation mode δ(HNH) is observed at 1,418 cm^{-1} [30, 45]. The Raman dispersion spectrum (Fig. 4) of the complex shows two strong CN bands in the region 2,000–2,200 cm^{-1} [46]. The band located at lower frequency is due to the CN symmetric stretching. In the IR spectrum, only one CN stretching band was observed. This result is in agreement with the selection rules showing that the vibration modes of A_{1g}, E_g and T_{1u} symmetry will be only Raman-active [47].

Figures 3 (II) and (III) show the IR spectra of the decomposition products of $Ba(NH_4)_2[Fe(CN)_6]\cdot 3H_2O$ at 450 °C and 1,000 °C, respectively. The ν_3(CN) stretching band located at 2,041 cm^{-1} at RT disappeared in both spectra, while at the same time, there appear bands corresponding to the presence of barium carbonate at 1,437, 857 and 686 cm^{-1} due to stretching of C=O and the angular deformations of the CO_3^{2-}, respectively [14, 15, 26, 45] (see Table 4).

This behavior agrees with the plateaus appearing around 400 °C and the last plateau from 700 °C in the TG measurement. The inset of Fig. 3 details the oxides spectral region between 600 and 250 cm^{-1}. The tentative assignment of the IR and Raman spectra is collected in Table 4.

Conclusions

The ammonium, barium hexacyanoferrate(II) trihydrate, $Ba(NH_4)_2[Fe(CN)_6]\cdot 3H_2O$, has been synthesized for the first time, was characterized by TG, IR and chemical analysis and its crystal and molecular structures were determined by X-ray diffraction methods. The compound crystallizes in the trigonal *R*-3*c* space group (in the hexagonal setting) with $a = b = 7.3744(2)$, $c = 45.758(2)$ Å and $Z = 6$ molecules per unit cell. In the lattice, Fe(II) ion is sited on a special position with point symmetry S_6 ($\bar{3}$) in a nearly perfect octahedral environment. The Ba(II) ion is located on a crystallographic D_3 point symmetry in a ninefold environment. It is coordinated by six cyanide groups conforming an Archimedean triangular anti-prism geometry, where the metal is sandwiched between two triangular basis with a cyanide N atom at each vertex [d(Ba–N) = 2.894(2) Å], rotated in 14.12(7)° from each other.

According to the thermal analysis, $Ba(NH_4)_2[Fe(CN)_6]\cdot 3H_2O$ decomposes in four steps. The first one corresponds to the elimination of three water molecules (coordinated water) per chemical formula, the second step is attributed to the loss of two ammonium cyanide molecules and the formation of iron(II) cyanide and barium cyanide. The third decomposition step is attributed to the elimination and oxidation of the CN groups with the simultaneous formation of barium carbonate and ferric oxide. Finally, in the last stage, it can be assumed that part of barium carbonate is decomposed to generate $BaFeO_{2.5}$ mixed oxide.

Supplementary information

Tables of fractional coordinates and equivalent isotropic displacement parameters of the non-H atoms (Table S5), atomic anisotropic displacement parameters (Table S6), Hydrogen coordinates and isotropic displacement parameters (Table S7) and H bond distances and angles (Table S8). A CIF file with details of the crystal structure reported in this paper has been deposited with the Cambridge Crystallographic Data Centre under deposition number CCDC 901579.

Acknowledgements This work was supported by CONICET (PIP 1529), and by ANPCyT (PME06 2804 and PICT06 2315) of Argentina. G.A.E. and O.E.P are Research Fellows of CONICET. L.M.C. and M.I.G. thank Consejo de Investigaciones de la Universidad Nacional de Tucumán (CIUNT) for financial support, Project 26D-517.

References

1. Wu L, Yu J, Zhang L, Wang X, Li S. Selective self-propagating combustion synthesis of hexagonal and orthorhombic nanocrystalline yttrium iron oxide. J Solid State Chem. 2004;177:3666–74.
2. Lu X, Xie J, Shu H, Liu J, Yin C, Lin J. Microwave-assisted synthesis of nanocrystalline YFeO3 and study of its photoactivity. Mater Sci Eng B. 2007;138:289–92.
3. Lentmaier J, Kemmier-Sack S, Knell G, Kessier P, Plies P. Selective reduction of nitrogen monoxide by catalysts based on composites between solid acid and perovskite in the presence of excess oxygen. Mater Res Bull. 1996;31:1269–76.
4. Lentmaier J, Kemmier-Sack S. Bifunctional $YFeO_3$-based catalysts used in the selective catalytic reduction of nitrogen monoxide in the presence of excess oxygen. Mater Res Bull. 1998;33:461–73.
5. Scott MJ, Holm RH. Molecular assemblies containing linear and Bent [Fe^{III}-CN-Cu^{II}] bridge units: synthesis, structure, and relevance to cyanide-inhibited heme-copper oxidases. J Am Chem Soc. 1994;116:11357–67.
6. Iwamoto T. Supramolecular chemistry in cyanometallate systems. In: Lehn JM. Comprehensive supramolecular chemistry. London: Pergamon; 1996.
7. Knoeppel DW, Shore SG. Cyanide-bridged lanthanide–transition metal one-dimensional arrays $\{(DMF)_{10}Yb_2[Ni(CN)_4]_3\}_\infty$ and $\{(DMF)_{10}Yb_2[Pt(CN)_4]_3\}_\infty$. Inorg Chem. 1996;35:1747–8.
8. Zhang HX, Tong YX, Chen ZN, Yu KB, Kang BS. Cyano-bridged extended heteronuclear supramolecular architectures with hexacyanoferrates(II) as building blocks. J Organomet Chem. 2000;598:63–70.
9. Černák J, Orendáč M, Potočňák I, Chomič J, Orendáčová A, Skoršepa J, Feher A. Cyanocomplexes with one-dimensional structures: preparations, crystal structures and magnetic properties. Coord Chem Rev. 2002;224:51–66.
10. Nakayama S, Sakamoto M, Matsuki K, Okimura Y, Ohsumi R, Nakayama Y, Sadaoka Y. Preparation of perovskite-type $LaFeO_3$ by thermal decomposition of heteronuclear complex, $\{La[Fe(CN)_6]\cdot 5H_2O\}_x$. Chem Lett. 1992;11:2145–7.
11. Matsuura Y, Matsushima S, Sakamoto M, Sadaoka Y. NO_2-sensitive $LaFeO_3$ film prepared by thermal decomposition of the heteronuclear complex, $\{La[Fe(CN)_6]\cdot 5H_2O\}_x$. J Matter Chem. 1993;3:767–9.
12. Sadaoka Y, Watanabe K, Sakai Y, Sakamoto M. Preparation of perovskite-type oxides by thermal decomposition of heteronuclear complexes, $\{Ln[Fe(CN)_6]\cdot nH_2O\}_x$, (Ln–La ~ Ho). J Alloys Compd. 1995;224:194–8.
13. Kondo N, Itoh H, Kurihara M, Sakamoto M, Aono H, Sadaoka Y. New high-yield preparation procedure of $Ln[Fe(CN)_6]\cdot nH_2O$ (Ln=La, Gd and Lu) and their thermal decomposition into perovskite-type oxides. J Alloys Compd. 2006;408:1026–9.
14. Gómez MI, de Morán JA, Carbonio RE, Aymonino PJ. Synthesis of $AFeO_{2.5+x}$ ($0 \le x \le 0{,}5$; A = Sr, Ca) mixed oxides from the oxidative thermal decomposition of $A[Fe(CN)_5NO]\cdot 4H_2O$. J Solid State Chem. 1999;142:138–45.
15. Gómez MI, de Morán JA, Aymonino PJ, Pagola S, Stephens P, Carbonio RE. Ab initio structure solution of $BaFeO_{2.8-\delta}$, a new polytype in the system of BaFeOy ($2.5 \le y \le 3.0$) prepared from the oxidative thermal decomposition of $BaFe[(CN)_5NO]\cdot 3H_2O$. J Solid State Chem. 2001;160:17–24.
16. Navarro MC, Pannunzio-Miner EV, Pagola S, Gómez MI, Carbonio RE. Structural refinement of $Nd[Fe(CN)_6]\cdot 4H_2O$ and study of $NdFeO_3$ obtained by its oxidative thermal decomposition at very low temperatures. J Solid State Chem. 2005;178:847–54.
17. Córdoba LM, Gómez MI, de Morán JA, Aymonino PJ. Synthesis of the $SrFeO_{2.5}$ and $BaFeO_{3-x}$ perovskites by thermal decomposition of $SrNH_4[Fe(CN)_6]\cdot 3H_2O$ and $BaNH_4[Fe(CN)_6]$. J Argent Chem Soc. 2008;96:1–2.
18. Gil DM, Navarro MC, Lagarrigue MC, Guimpel J, Carbonio RE, Gómez MI. Synthesis and structural characterization of perovskite $YFeO_3$ by thermal decomposition of a cyano complex precursor, $Y[Fe(CN)_6]\cdot 4H_2O$. J Therm Anal Calorim. 2011;103:889–96.
19. Gil DM, Guimpel J, Paesano A Jr, Carbonio RE, Gómez MI. $Y[Fe_{1-x}Co_x(CN)_6]\cdot 4H_2O$ ($0 \le x \le 1$) solid solutions: synthesis, crystal structure, thermal decomposition and spetroscopic and magnetic properties. J Mol Struct. 2012;1015:112–7.
20. Gil DM, Navarro MC, Lagarrigue MC, Guimpel J, Carbonio RE, Gómez MI. Crystal structure refinement, spectroscopic study and magnetic properties of yttrium hexacyanoferrate(III). J Mol Struct. 2011;1003:129–33.
21. Kumar Swamy N, Pavan Kumar N, Venugopal Reddy P, Manish Gupta, Shanmukharao Samatham S, Venkateshwarulu D, Ganesan V, Vikas Malik, Das BK. Specific heat and magnetocaloric effect studies in multiferroic $YMnO_3$. J Therm Anal Calorim. 2014. doi:10.1007/s10973-014-4223-3.
22. Bailey WE, Williams RJ, Milligan WO. The crystal structure of $La[Fe(CN)_6]\cdot 5H_2O$. Acta Crystallogr B. 1973;29:1365–8.
23. Kietaibl H, Petter W. Die Kristallstrukturen von $La[Fe(CN)_6]\cdot 5H_2O$ und $Sm[Fe(CN)_6]\cdot 4H_2O$. Helv Phys Acta. 1974;47:425.
24. Bonnet MC, Paris RA. Hexacyanometallates: part 1: radiographic and infrared study of lanthanide hexacyanoferrates(III). Bull Soc Chim Fr. 1975;5–6:1062–6.

25. Bonnet MC, Paris RA. Lanthanide hexacyanometallates: part 2: radiocrystallographic and infrared study of lanthanide hexacyanocobaltates(III) thermal decomposition. Bull Soc Chim Fr. 1975;5–6:1067–70.
26. Navarro MC, Lagarrigue MC, De Paoli JM, Carbonio RE, Gómez MI. A new method of synthesis of $BiFeO_3$ prepared by thermal decomposition of $Bi[Fe(CN)_6]\cdot 4H_2O$. J Therm Anal Calorim. 2010;102:655–60.
27. Navarro MC, Lagarrigue MC, Carbonio RE, Gómez MI. Synthesis, characterization and study of products of the thermal decomposition of $Bi[Fe_xCo_{1-x}(CN)_6]\cdot 4H_2O$. Glob J Inorg Chem. 2010;1:76–82.
28. Gil DM, Ávila M, Reguera E, Pagola S, Gómez MI, Carbonio RE. Lead hexacyanoferrate(II) tetrahydrate: crystal structure, FTIR spectroscopy and thermal decomposition studies. Polyhedron. 2012;33:450–5.
29. Raistrick ID, Endow N, Lewkowitz S, Huggins RA. Structural aspects of some mixed metal ferrocyanides. J Inorg Nucl Chem. 1977;39:1779–83.
30. Medina Córdoba L, de Morán JA, Santos S Jr, Piro OE, Gómez MI. Synthesis and crystal structure of ammonium, strontium hexacyanoferrate(II) dihydrate. J Chem Crystallogr. 2011;41:1280–6.
31. Gallagher PK. A simple technique for the preparation of R.E. FeO_3 and R.E. CoO_3. Mater Res Bull. 1968;3:225–32.
32. Traversa E, Nunziante P, Sakamoto M, Sadaoka Y, Carotta MC, Martinelli G. Thermal evolution of the microstructure of nanosized $LaFeO_3$ powders from the thermal decomposition of a heteronuclear complex, $La[Fe(CN)_6]\cdot 5H_2O$. J Mater Res. 1998;13:1335–43.
33. Gil DM, Carbonio RE, Gómez MI. Synthesis of $Pb_2Fe_2O_5$ by thermal decomposition of $Pb_2[Fe(CN)_6]\cdot 4H_2O$. J Chil Chem Soc. 2010;55(2):189–92.
34. Navarro MC, Lagarrigue MC, De Paoli JM, Carbonio RE, Gómez MI. Synthesis and structural characterization of perovskite $YFeO_3$ by thermal decomposition of a cyano complex precursor $Y[Fe(CN)_6]\cdot 4H_2O$. J Therm Anal Calorim. 2010;102:655–60.
35. Williams HE. Cyanogen compounds. London: Arnold; 1948.
36. Ayres GH. Análisis químico cuantitativo. Spain: Harper & Row Inc; 1991.
37. Rodier J. Análisis de las aguas. Barcelona: Omega SA; 1978.
38. Vogel I. Química analítica cuantitativa. Argentina: Kapelusz; 1969.
39. CrysAlisPro, Oxford Diffraction Ltd., version 1.171.33.48 (release 15-09-2009 CrysAlis171.NET).
40. Sheldrick GM. A short history of SHELX. Acta Crystallogr A. 2008;64:112–22.
41. Hurlbut CS, Klein C Jr. Manual de minerología. 4ª ed. España: Reverté SA; 1997.
42. Johnson CK. ORTEP-II: a Fortran Thermal-Ellipsoid Plot Program. Report ORNL-5318, Oak Ridge National Laboratory, Tennessee, USA, 1976.
43. Lide DR. Handbook of chemistry and physics. 80th Ed. New York: Chemical Rubber Publishing Company; 1999–2000.
44. Deb N. The solid state thermal decomposition of $Sr_3[La(C_2O_4)_3(H_2O)_2]_2\cdot 11H_2O$. J Therm Anal Calorim. 2012;114(1):261–7.
45. Nakamoto K. Infrared and Raman spectra of inorganic and coordination compounds. New York: Wiley; 1986.
46. Gil DM, Carbonio RE, Gómez MI. Crystal structure refinement and vibrational analysis of $Y[Co(CN)_6]\cdot 4H_2O$ and its thermal decomposition products. J Mol Struct. 2013;104:23–8.
47. Park S-K, Lee C-K, Lee S-H, Lee N-S. Vibrational analysis of ferrocyanide complex ion based on density functional force field. Bull Korean Chem Soc. 2002;23(2):253–61.